# Geometrical Dependence of High-Bias Current in Multiwalled Carbon Nanotubes

B. Bourlon,[1] D. C. Glattli,[1,2] B. Plaçais,[1] J. M. Berroir,[1] C. Miko,[3] L. Forró,[3] and A. Bachtold[1,*]

[1]*Laboratoire de Physique de la Matière Condensée de l'Ecole Normale Supérieure, 24 rue Lhomond, 75231 Paris 05, France*
[2]*SPEC, CEA Saclay, F-91191 Gif-sur-Yvette, France*
[3]*EPFL, CH-1015, Lausanne, Switzerland*
(Received 30 May 2003; published 14 January 2004)

We have studied the high-bias transport properties of the different shells that constitute a multi-walled carbon nanotube. The current is shown to be reduced as the shell diameter is decreased or the length is increased. We assign this geometrical dependence to the competition between the electron-phonon scattering process and Zener tunneling.

PACS numbers: 73.63.Fg, 72.10.Di, 73.50.Fq

Building electronic devices at the molecular scale has motivated intense research for the past few years. Carbon nanotubes have been used as building blocks for devices such as nanotube-nanotube junctions [1,2] or field-effect transistors [3,4] that have been integrated in logic circuits [5–7]. Recently, nanotubes have also attracted widespread attention as future interconnects [8–11], since their current-carrying capacities are several orders of magnitude larger than in present-day interconnects. The current in metal single-wall nanotubes (SWNT) saturates at 20–25 $\mu$A, which corresponds to a current density exceeding $10^9$ A/cm$^2$ [12].

An important question that remains to be addressed is how the current saturation grows with the section of an interconnect made of SWNTs. An approach for larger interconnect is to select multiwalled nanotubes (MWNTs) with many concentric shells. Recently, Collins *et al.* have shown [13,14] that most of the shells contribute to the current at large bias [15] and that the current of each shell saturates as in SWNTs. The saturation value was reported to be identical for the different shells of a MWNT. The measurements were done on thin-diameter MWNTs contacted by electrodes separated by ~200 nm.

In this Letter, we present studies of the high-bias transport carried on larger diameter MWNTs and with different electrode separations $L$. We find that the current saturation per shell varies between 10 and 60 $\mu$A. For the shortest separation (200 nm), the current is shown to increase as a function of diameter. For longer separations (1 $\mu$m), the diameter dependence is much weaker and more difficult to observe. We propose that this geometrical dependence is due to a weak variation of the number of current-carrying subbands within each shell. This results from the competition in the electron transmission between the electron-phonon scattering process and Zener tunneling. The Landauer formula is applied that incorporates these two processes, and the numerical calculations reproduce well the experimental results. Interestingly, the model describes the experimental observation that the high-bias current does not depend on

the metal or the semiconducting character of the shell at large diameters.

The MWNTs were synthesized by arc-discharge evaporation and carefully purified [16]. The MWNTs are sonicated in dichloroethane and dispersed onto an oxidized Si substrate. Atomic force microscopy is used to image, select, and locate nanotubes that are then contacted with Cr/Au electrodes by electron beam lithography. An example of a device is shown in Fig. 1(a). Typical two-point resistances at low-bias vary in the range 5 to 30 k$\Omega$.

The electronic properties of different shells in a MWNT are probed using the electrical-breakdown method [13,14]. The shells are selectively removed step-wise by injecting a large current in the MWNT. The bias voltage is increased until a sharp step in the current is detected that corresponds to the failure of one shell. Then, the bias voltage is quickly put down to 0 in 100 ms. The removed shell has been shown to be the outermost one which is in direct contact with air and therefore most subject to a rapid oxidation initiated by the current [14]. We remove shells until no more current is detected. The final diameter has then decreased to typically 2–4 nm as seen on the AFM picture in Fig. 1(b). The image shows that the peeling is uniform along the tube, except near the electrodes. Note that the failure is apparently different for the last shells since they are not evaporated. Failure may be local and situated at a small gap, too short to be observed with AFM.

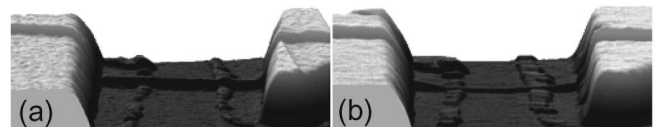We have designed an experiment where a series of electrodes is attached to a single long MWNT with



FIG. 1. AFM image of a MWNT (a) before and (b) after the application of the electrical-breakdown method. $d$ has been reduced from 12 to 3 nm. $L = 600$ nm and the electrode height is 45 nm. Residual lithography resist is observed to follow the electrode edges.

various separations from 200 to 1200 nm. The diameter $d$ measured by AFM is 15 nm. The uniform $d$ suggests a constant number of shells along the whole MWNT. Figures 2(a)–2(c) show the result of the electrical-breakdown method applied to the different sections of this MWNT. Let us first consider the current-voltage characteristics ($I$-$V$) of the pristine sample given by the upper $I$-$V$ curve. It appears that the high-bias current is significantly larger in the shortest section. This result can be enlightened by analyzing the $I$ carried by the different shells of the MWNT that are obtained by comparing the successive $I$-$V$. Inspection of Figs. 2(a)–2(c) shows that the large $I$ obtained for the shortest section is the combined effect of (i) more jumps and (ii) larger jumps.

We discuss first the jump number. This 15 nm diameter MWNT is expected to consist of ∼19 shells. The jump number is, however, smaller and $L$ dependent. It is reduced from 17 to 13 when $L$ passes from 200 to 1200 nm. This suggests that some shells do not participate to $I$, especially in the longer sections. Such an interpretation is supported by the following observation in Fig. 2(d), where the maximum current $I_{\max}$ of each $I$-$V$ is plotted as a function of $d$. The diameter has been estimated by subtracting from the 15 nm diameter pristine MWNT twice the interlayer distance 3.4 Å for each removed shell. Height measurements with AFM on other samples agree with such a $d$ estimation. The figure shows that the $I_{\max}(d)$ curve is abruptly finished at thin diameters. The last jump is much larger and corresponds to the failure of several
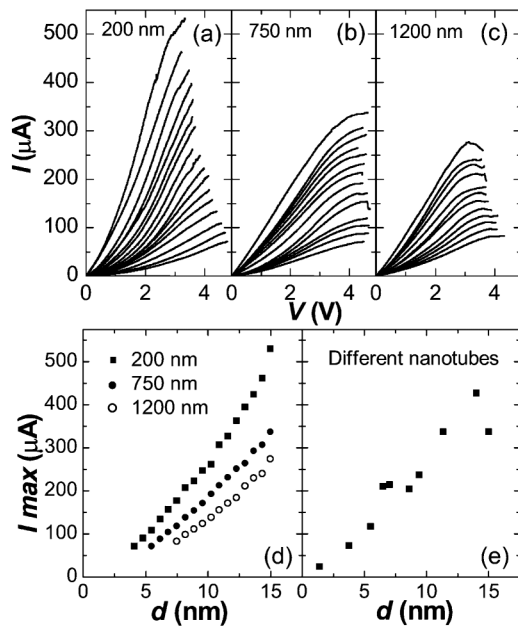
shells. The extrapolated curves should pass by 25 $\mu$A at 1.4 nm, the saturation of a SWNT. This is not the case. Rather, the extrapolations have negative $I$ values at 1.4 nm, which indicates that some thin-diameter shells do not participate to $I$.

As mentioned previously, the current jumps for the shortest length are larger in amplitude. The jump averages are 28.7, 19.1, and 17.4 $\mu$A for, respectively, the 200, 750, and 1200 nm lengths. Remarkably, the curves in Fig. 2(d) deviate from a linear behavior. The deviation is best seen for the 200 nm length. It shows that large-diameter shells contribute more to $I$. This finding has been observed in more than 20 MWNTs. Other examples are shown in Figs. 3(a) and 3(b), where the current jump $\Delta I$ is plotted as a function of $d$. Both curves show that $\Delta I$ is larger for larger $d$. However, the slope is much weaker for the 650 nm length and is hardly observed due to the measurement noise.

We note that an accurate determination of $\Delta I$ is difficult. The inset of Fig. 3(a) shows that the bias at which the shell fails increases irregularly and that the $I$-$V$ are not smooth. We define $\Delta I$ as the current difference at a bias $V_0$ given by the maximum voltage recorded for the two successive $I$-$V$. Another approach could have been to take the maximum of the difference or the difference of the maximums. However, the observation of a current increase with $d$ is not altered by the choice of the estimation procedure. Importantly, the $\Delta I$ estimation is
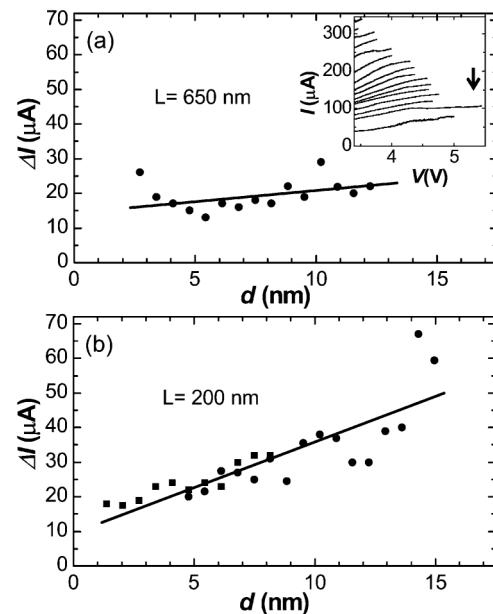


FIG. 2. (a)–(c) High-bias $I$-$V$ characteristics of the same 15 nm diameter MWNT with different $L$. Each $I$-$V$ corresponds to the loss of one shell. The 11th $I$-$V$ in (b) and the 5th $I$-$V$ in (c) could not be recorded. The $I$-$V$ have been measured at 300 K in air. (d) $I_{\max}$ as a function of $d$ from (a)–(c). (e) $I_{\max}$ as a function of diameter for different MWNTs. $L$ is between 500 and 750 nm.



FIG. 3. High-bias jump of $I$ as a function of $d$ for (a) 650 nm and (b) 200 nm lengths. The points in (b) around 60–70 $\mu$A might be an artifact resulting from two failures. However, other samples have shown a nice continuous increase between 40 and 60 $\mu$A, which suggests that such large $I$ are obtained for single shells. The straight lines are guides for the eyes. (b) shows the data of two samples represented by squares and dots. The inset of (a) shows the $I$-$V$. The arrow indicates an $I$-$V$ discussed in the text.

precise enough to obtain close slopes of $\Delta I(d)$ for different MWNTs with the same length as seen in Fig. 3(b).

We now discuss the possible origins of these geometrical dependencies in $\Delta I$. It might be related to heating. Shorter and larger shells might be better heat sunk to the electrodes. However, it has already been shown in SWNTs that current saturation is both length and temperature independent [12] and thus not sensitive to heating. There is no reason to expect a different behavior in MWNTs since similar $I$ and $V$ are obtained at saturation. Another argument might be that heating affects the failure voltage below saturation. This premature failure occurs essentially in the shortest section contrary to what is expected with heating [Figs. 2(a)–2(c)].

Now, we review the electron-phonon scattering process that causes $I$ to saturate at 20–25 $\mu$A in metal SWNTs [12]. An electron that is accelerated by an electric field $\mathcal{E}$ will gain energy until an optical phonon of energy $\hbar\Omega$ is emitted ($\hbar\Omega \approx 0.16$ eV) and will be backscattered. The mean-free path $l_{ph}$ is equal to the distance an electron must travel to be accelerated to $\hbar\Omega$, $l_{ph} = \hbar\Omega/e\mathcal{E}$ [12]. The total transmission through the whole tube is obtained by dividing $l_{ph}$ by $L$:

$$T_{ph} = \hbar\Omega/eV, \qquad (1)$$

where $V$ is the voltage applied between the electrodes. Equation (1) is valid only for large $V$.

The $\Delta I$ variations might be explained from the energy variation of phonons as a function of $d$. However, *ab initio* calculations have shown that optical phonon energy changes barely with $d$ [17]. Another mechanism is thus needed to account for the $\Delta I$ variation.

We propose that the $\Delta I$ sensitivity to $d$ results from the contribution of Zener tunneling [18]. Figure 4(a) shows a scheme that represents the potential variation in space of the band structure. The potential drop should be in principle determined by the self-consistent solution of the Poisson equation and the nonequilibrium electron density. We assume here that the voltage drop is linear, a good approximation when multiple electron-phonon scattering processes occur [19].

An electron that enters a noncrossing subband from the left electrode reaches at some point the top of the valence band and tunnels to the conduction band. The Zener-tunneling transmission [20] is given by

$$T_Z = \exp\left(-\frac{4\sqrt{2m^*}LE^{3/2}}{3e\hbar V}\right), \qquad (2)$$

where we have assumed a linear voltage drop. $m^*$ is the effective mass and $E$ the gap that goes similar to $1/d$.

Now, we compare $T_{ph}$ and $T_Z$ as a function of $d$. $T_{ph}$ is independent on $d$ and $T_{ph} = 0.045$ at 3.5 V. For a large semiconducting shell of 15 nm diameter and $L = 200$ nm, we obtain $T_Z \approx 0.7$ for tunneling between the upper valence band and the lower conduction band. The effective mass has been estimated using the tight-binding model for a zigzag tube. The comparison between $T_{ph}$
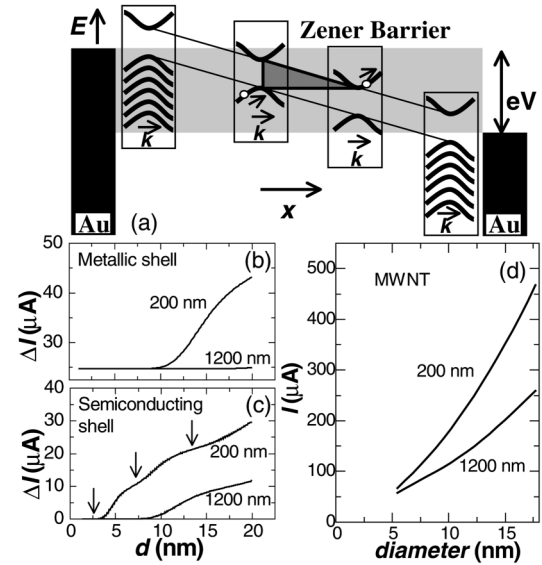


FIG. 4. (a) Schematic of the potential variation in space. The boxes show the band diagram of a semiconducting shell. The Zener barrier is indicated by the triangle. Numerical calculations of $I$ for (b) metal and (c) semiconducting shells at 3.5 V and for two $L$. $I = 25$ $\mu$A at $d = 0$ in metal shells because of the two crossing bands where the Zener barrier is absent. The arrows indicate plateaus where 0, 1, and, respectively, 2 subbands carry current. (d) Calculated $I$ of a MWNT as a function of diameter.

and $T_Z$ shows that the current is limited by phonons. Zener reflection is here unimportant and no difference in current is expected between metal and semiconducting shells in agreement with experiment. The situation changes for small-diameter shells. For $d = 3$ nm, we estimate $T_Z \approx 10^{-4}$ so that the current is now limited by Zener tunneling [21].

Here, we discuss the contributions of the other subbands. The gap is larger and $T_Z$ lower. For the 15 nm diameter shell, we estimate $T_Z \approx 0.2$ and $4 \times 10^{-3}$ for the second and third subbands. We obtain for $d = 3$ nm, $T_Z \approx 2 \times 10^{-15}$ for the second subband. The subbands that carry current have $T_Z(E) > T_{ph}$, which shows that very few subbands within a shell contribute. Moreover, their number $N$ varies weakly with $d$. We have for semiconducting shells $N = 2$ for $d = 15$ nm and $N = 0$ for $d = 3$ nm. This implies that the current jump changes weakly with $d$ in agreement with experiment.

To put the above analysis on a more quantitative basis, we use the Landauer formula to estimate the high-bias current of a shell. Since the transmissions are weak, the total transmission of the subband $i$ is given by $T_i^{-1} = T_Z^{-1}(E_i) + T_{ph}^{-1}$. $E_i$ is the energy separation between the $i$ valence band to the $i$ conduction band, where $i$ is counted from the neutrality point. Note that alternative processes such as tunneling from the $i$ valence band to the first conduction band changes barely the results presented below. $I$ is given by $(2e/h)\int\sum_i T_i\,dE$. The integral is calculated between 0 and $eV$. The use of the Landauer

formula in the presence of inelastic scattering in the nonequilibrium regime is rather crude since it does not account for the exclusion principle. It allows one to give some physical insight. A model based on the Boltzmann equation as in [12] that incorporates Zener tunneling is probably needed for more accuracy.

Figures 4(b) and 4(c) show the calculated $I$ as a function of $d$ of metal and semiconducting shells. $I$ increases with $d$ and decreases with $L$, in agreement with experiment. Indeed, larger diameters decrease the subband gap and enable better Zener transmission. Similarly, the tunneling transmission becomes weaker for longer nanotubes as the Zener barrier length increases [Fig. 4(a)].

Figure 4(d) shows the calculated $I$ as a function of the diameter $D$ of MWNTs. We assume that MWNTs consist of shells that carry current in parallel. The current through the MWNT is the sum of the current of a series of shells with $d$ ranging from 2 nm to $D$. For each shell, an average is taken on the current of a semiconducting and a metal shell with the statistical weights $\frac{2}{3} - \frac{1}{3}$. The resemblance to the experiment is remarkable. *No fitting parameter has been used.*

Figure 4(c) shows $I$ of semiconducting shells as a function of $d$. It appears that thin-diameter shells do not carry current. This happens when $T_Z(E) < T_{ph}$. Moreover, the diameter at which semiconducting shells start to conduct becomes larger for longer tubes, since $T_Z(E)$ decreases with $L$. This may explain the discussed experimental observation that the number of jumps is reduced for the longer section. Such an interpretation is further supported as follows. The inset of Fig. 3(a) shows that the $I$-$V$ indicated by an arrow fails at a bias larger than the others. Such $I$-$V$ have been observed several times but mostly for the last $I$-$V$. At the failure, the current is typically 50–100 $\mu$A and corresponds to several shells. We propose that the outermost shell is semiconducting in this situation and does not carry current. The current has to pass through inner shells that are protected from oxygen and that can sustain higher voltages. At the failure, the breakdown is mostly so violent that all the shells fail together.

Here, we discuss the role of disorder that can backscatter electrons. Some experiments [22] have reported that MWNTs are ballistic, but previous measurements [23] on similarly prepared samples have given an elastic length $L_e$ due to disorder around ~100 nm. The corresponding transmission for a 200 nm long tube is $L_e/L \approx 1/2$, which is larger than $T_Z$ and $T_{ph}$. Impurities in short shells are thus unimportant, but may become relevant for the much longer ones.

We finish with a discussion on the performances of large-diameter MWNTs as interconnects. We have shown that the number of current-carrying subbands within a shell depends weakly on $d$ and $L$ and stays typically close to 1. Thus, the current saturation of MWNTs is expected to vary roughly linearly with the shell number and, thus,

the diameter. This is observed in Fig. 2(e), where $I_{max}$ as a function of $d$ is plotted for ten samples. The functional form is not quadratic as would be expected for a plain wire. This makes current-carrying capacities of MWNTs less efficient as interconnects when they become larger. However, the current-carrying capacity of large MWNTs still surpasses Cu wires ($\approx 10^6$ A/cm$^2$). For example, $I$ of a 100 nm diameter MWNT is estimated to be 10–100 times larger.

*Author to whom correspondence should be addressed.
Electronic address: bachtold@lpmc.ens.fr
[1] M. S. Fuhrer *et al.*, Science **288**, 494 (2000).
[2] Z. Yao, H. W. C. Postma, L. Balents, and C. Dekker, Nature (London) **402**, 273 (1999).
[3] S. J. Tans, A. R. M. Verschueren, and C. Dekker, Nature (London) **393**, 49 (1998).
[4] R. Martel *et al.*, Appl. Phys. Lett. **73**, 2447 (1998).
[5] A. Bachtold, P. Hadley, T. Nakanishi, and C. Dekker, Science **294**, 1317 (2001).
[6] V. Derycke, R. Martel, J. Appenzeller, and P. Avouris, Nano. Lett. **1**, 453 (2001).
[7] X. Liu *et al.*, Appl. Phys. Lett. **79**, 3329 (2001).
[8] P. L. McEuen, M. S. Fuhrer, and H. Park, IEEE Trans. Nanotech. **1**, 78 (2002).
[9] B. Q. Wei, R. Vajtai, and P. M. Ajayan, Appl. Phys. Lett. **79**, 1172 (2001).
[10] F. Kreupl *et al.*, Microelectron. Eng. **64**, 399 (2002).
[11] J. Li *et al.*, Appl. Phys. Lett. **82**, 2491 (2003).
[12] Z. Yao, C. L. Kane, and C. Dekker, Phys. Rev. Lett. **84**, 2941 (2000).
[13] P. G. Collins, M. S. Arnold, and Ph. Avouris, Science **292**, 706 (2001).
[14] P. G. Collins *et al.*, Phys. Rev. Lett. **86**, 3128 (2001).
[15] This is in contrast to low-bias and low-temperature measurements. A. Bachtold *et al.*, Nature (London) **397**, 673 (1999).
[16] J. M. Bonard *et al.*, Adv. Mater. **9**, 827 (1997).
[17] O. Dubay and G. Kresse, Phys. Rev. B **67**, 035401 (2003).
[18] M. P. Anantram, Phys. Rev. B **62**, R4837 (2000).
[19] The voltage drops are neglected at the nanotube-electrode interface. Indeed large contact resistances are observed to have no influence on the current saturation.
[20] S. M. Sze, in *Physics of Semiconductors Devices* (Wiley Interscience, New York, 1981).
[21] For $d = 15$ nm, $E = 53$ meV and $m^* = 6.5 \times 10^{-33}$ kg. For $d = 3$ nm, $E = 270$ meV and $m^* = 2.8 \times 10^{-32}$ kg.
[22] S. Frank *et al.*, Science **280**, 1744 (1998).
[23] C. Schönenberger *et al.*, Appl. Phys. A **69**, 283 (1999); A. Bachtold *et al.*, Phys. Rev. Lett. **84**, 6082 (2000).